Magnetic peptide nucleic acids for DNA targeting†

Giuseppe Prencipe,[a] Stefano Maiorana,[a] Paolo Verderio,[a] Miriam Colombo,[b] Paola Fermo,[c] Enrico Caneva,[d] Davide Prosperi*[b] and Emanuela Licandro*[a]

Received (in Cambridge, UK) 11th June 2009, Accepted 4th August 2009
First published as an Advance Article on the web 20th August 2009
DOI: 10.1039/b911449a

A versatile synthetic platform for the efficient immobilization of PNAs on magnetic iron oxides, providing magnetic nanosensors for selective DNA recognition, is presented.

Peptide nucleic acids (PNAs) are mimics of natural oligonucleotides, in which each ribose phosphate unit is replaced by an aminoethylglycine unit.[1] The nucleobases are appended to the backbone aminoethylglycine nitrogens through a methylene-carbonyl group. PNAs bind complementary DNA and RNA strands with excellent affinity and sequence specificity due to the absence of electrostatic interference of their neutral chain with polyanionic oligonucleotide backbone. In addition, PNAs exhibit greater mismatch selectivity and chemical and enzymatic stability compared to natural oligonucleotides. All of these features have attracted significant interest, which has arisen in view of their potential in gene diagnosis and therapy. However, the first generation of PNAs suffers from some drawbacks, which hamper the full exploitation of them in gene therapy, including low cell uptake and some low solubility in physiological media. To overcome these problems, and to improve their physical–chemical properties, many modified PNAs have been synthesized in recent years following different strategies.[2] Along with the recent advances in DNA technology,[3] the integration with nanostructured systems is expected to improve PNA properties and applicabilities.

In this context, superparamagnetic iron oxide nanoparticles (MNP) attracted our attention because of their unique magnetic properties, which can be controlled rigorously and activated easily by applying an external magnetic field.[4] In most cases, specific surface biofunctionalization is required for the successful utilization of MNP in biomedicine. Many effective applications of MNP have been described so far, including the selective separation of biomolecules and cells,[5] automated DNA extraction,[6] targeted gene delivery,[7] use as magnetic resonance contrast agents (MRI),[8] and magnetic field induced hypertermia for cancer therapy.[9]

In several instances, single-stranded DNA was successfully supported on MNP and tested in hybridization experiments and single-nucleotide polymorphism analysis.[10] In contrast, PNAs have been seldom considered and, to our knowledge, only two examples have been reported so far. In the first study, PNA was connected to the γ-Fe_2O_3 MNP by exploiting the largely adopted thiol chemistry. Hybridization and mismatch experiments with ssDNA were conducted by surface-enhanced Raman scattering (SERS).[11] More recently, the synthesis of gold coated cobalt ferrite MNP functionalized with thiol-PNAs was reported.[12] However, we are aware that the interest in MNP-conjugated PNAs (MPNA) could spread well beyond this preliminary information, eventually conditioning the potential of PNA in biology and medicine. Several PNA applications, which are characteristic of DNA technology, would benefit from such an innovation, including cell uptake and site-directed delivery, use as antigene and antisense therapeutic agents, control on the size and morphology of nanoconjugates, and use as biosensors through the rapid and reliable assessment of DNA hybridization by T_2 relaxation measurements complemented by conventional determination of the melting temperature of hybrids.

In this note, we describe a versatile, effective synthetic platform for the development of monomer and decamer PNA-nanoconjugates, starting from synthetic PNA and nanometer-sized maghemite. The sequence-selective DNA recognition and sequestration ability of the resulting MPNA were assessed according to their capability of enhancing the T_2 relaxation response in aqueous solutions under conventional hybridization conditions with complementary DNA.

We have used nearly homogeneous commercial γ-Fe_2O_3 nanoparticles (10 ± 4 nm), approximately spherical in shape, as observed by TEM. We chose the thymine monomer as a model PNA building unit for our study. First, we designed a small library of PNA monomer derivatives endowed with three different appropriate linkers useful for MNP conjugation. In particular, we synthesized the functionalized monomers **1–4** (Scheme 1, see ESI for experimental details). The trialkoxysilane, the carboxyl, and the propargylic groups are all suitable linkers to stably connect biomolecules to MNP through the formation of different kinds of linkages.[13–15] Such linkers, however, have never been applied to PNA for MNP conjugation. Monomer **4** was synthesized by the reaction of the terminal free amine of the methyl ester-protected thymine monomer **5** with 3-(triethoxysilyl)propyl isocyanate. PNA monomer **5** was also reacted with an equimolar amount of succinic anhydride providing **2** in excellent yield. Monomer **2**

[a] *Dipartimento di Chimica Organica e Industriale, Università di Milano, Via Venezian, 21-20133 Milano, Italy. E-mail: emanuela.licandro@unimi.it; Fax: (+39) 02503 14139; Tel: (+39) 02503 14143*
[b] *Dipartimento di Biotecnologie e Bioscienze, Università di Milano-Bicocca, P.zza della Scienza, 2-20126 Milano, Italy. E-mail: davide.prosperi@unimib.it; Fax: (+39) 026448 3565; Tel: (+39) 026448 3302*
[c] *Dipartimento di Chimica Inorganica, Metallorganica e Analitica, Università di Milano, Via Venezian, 21-20133 Milano, Italy*
[d] *Centro Interdipartimentale Grandi Apparecchiature (CIGA), Università di Milano, Via Golgi, 19-20133 Milano, Italy*

† Electronic supplementary information (ESI) available: Detailed experimental procedures, HRMAS NMR spectra, FTIR spectra, supplementary data. See DOI: 10.1039/b911449a

was subsequently reacted with propargylamine in the presence of EDC·HCl in DMF, affording **3** in good overall yields. Analytical and spectroscopic data, including elemental C,H,N analysis (EA), ^{1}H, ^{13}C and heteronuclear multiple quantum coherence (HMQC) NMR, and HR-ESI mass spectra, were in accordance with the expected structures for compounds **2–4** (see ESI for details†).

Scheme 1 illustrates the conjugation strategies exploited for the preparation of MPNA monomers and decamers. Monomers **1** and **2** were able to interact directly with nanoparticles through their carboxylate linkers. Similarly, compound **4** could be anchored to MNP effectively as a consequence of the high affinity of siloxane group for iron oxide. Compared to the carboxylate interaction, siloxane group provides a more stable, substantially irreversible, grafting to MNP surface. The functionalized nanoparticles were isolated by centrifugation and carefully washed affording **6–8**. The propargyl-terminating monomer **3**, was instead conjugated to the nanoparticles *via* a Cu(I)-catalyzed azide-alkyne "click" reaction with a MNP-silylpropylazide adduct, affording **9**. MNP-silylpropylazide was prepared according to our recently developed procedure.[15]

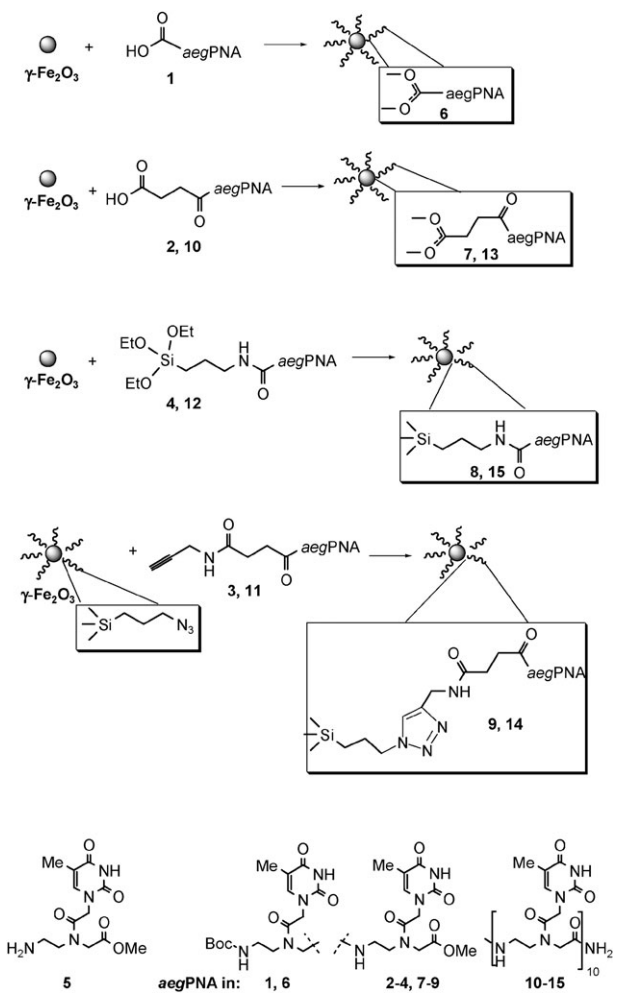

Scheme 1 Preparation of MNP-*aeg*PNA nanoconjugates: *aeg*PNA can either indicate PNA monomers (**1–4**) or 10-mers (**10–12**).

The organic structures of magnetic products **6–9** were completely characterized by FT-IR (bulk in KBr) and by high-resolution magic angle spinning (HR-MAS) NMR, which has been recently used to analyze bioconjugates of organic ligands with MNP.[14,15] Inductively coupled plasma spectroscopy (ICP-OES) analysis gave the content of iron isotopes in a sample of functionalized MNP, whereas EA provided quantitative data on the amount of organic material in the sample.

Homo-thymine 10-mer PNA was obtained by standard procedures (see ESI†) and functionalized with the above mentioned three linkers already explored with monomers. Three representative substituted 10-mers, **10–12**, were then grafted to MNP as reported in Scheme 1. Passive adsorption of the carboxyl derivative **10** gave **13**, while the formation of a stable covalent bond generated by "click" reaction of azide-MNP with the propargyl derivative **11** led to the MPNA **14**. Compound **12** could be effectively anchored onto MNP surface through a siloxane bridge with iron oxide, affording **15**. The nanoconstructs **13–15** were isolated by centrifugation and carefully washed with water to completely remove the unreacted excess of decamers **10–12**. MPNA nanohybrids **13–15** were characterized by FT-IR, demonstrating the presence of PNA on nanoparticles, while EA and ICP-OES provided information on the average amount of PNA decamers **10–12** on the nanoparticles. These data were compared with our calculations of the mass of a single MNP, therefore providing a reasonable hypothesis on the average loading of organic molecules on MNP. The results for the magnetic monomer and decamer thymine derivatives (**6–9** and **13–15**, respectively) are reported in Table 1. As expected, the carboxyl anchor allowed MNP to accommodate a larger number of PNA molecules on the same surface area.

Once a reliable, multiple-approach synthetic platform for the production of MPNA was optimized, the next objective was to determine the capability of these MPNA to recognize and bind the complementary DNA. On the basis of the fact that the formation of magnetic aggregates would result in a detectable increment in the T_2 relaxation time of water protons,[3,15,16] we decided to determine whether a variation of T_2 of MPNA could occur under MPNA/DNA hybridization conditions, and could be sensitively detected by relaxometric analysis (Fig. 1). In fact, a homo-thymine PNA decamer is documented to form a triplex of $(PNA)_2$/DNA type in the presence of complementary homo-adenine DNA strands. Therefore, we expected that the binding of homo-thymine MPNA to complementary homo-adenine DNA would result in the formation of aggregates associated with an increase of

Table 1 Average PNA numbers of molecules on single magnetic nanoparticle

MPNA	PNA molecule/NP
6	1660
7	4850
8	840
9	140
13	330
14	45
15	500

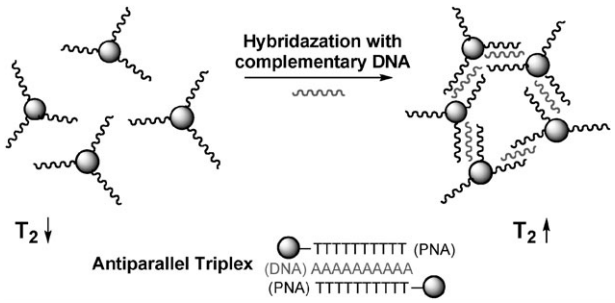

Fig. 1 Schematic MPNA clustering triggered by antiparallel triplex formation induced by DNA hybridization.

the detected T_2 value. Hence, we performed a set of experiments aimed at determining the efficiency and selectivity of MPNA in binding complementary DNA. First, a suitable concentration of MPNA **13** was determined in order to obtain an initial T_2 value within the range 100–200 ms (Fig. S3 in the ESI†). We found an optimal concentration of 13 μg Fe per mL. Concomitantly, the T_2 measurements in dependence of iron concentration were exploited to evaluate the magnetic relaxivity and the signal stability (inferred by the R^2 value of the relaxivity curve). Magnetic relaxivity was obtained by plotting $1/T_2$ as a function of iron concentration, giving an r_2 of 55.9 mM^{-1} s^{-1}, with an $R^2 > 99\%$, thus confirming a remarkable stability of the experimental magnetic environment (Fig. S4 in the ESI†). Next, we analyzed the change in T_2 as an effect of the hybridization of MPNA with complementary DNA (12.8 μg/mL) and compared it with two control cases: (1) absence of DNA, and (2) reaction with unmatched homo-thymine ssDNA. The results are illustrated in Fig. 2A, while the experimental procedure is reported in the ESI. The increment in T_2 with homo-adenine DNA (94%) as a consequence of MNP clustering owing to $(PNA)_2$/DNA matching is remarkably higher than in the control cases (2 *vs.* 1 and 3, Fig. 2A), for which the observed small residual increment can be accounted for by the adjustment due to temperature influence, with both being in the 10–20% range of increment. This experiment provides compelling evidence that the MPNA maintains both elevated and selective affinity for complementary DNA.

To confirm the ability of MPNA to recognize and bind the complementary DNA decamer, we have also acquired a melting curve of the hybrid formed between MPNA **13** and homo-adenine ssDNA (both at a concentration of 2.5 μM).

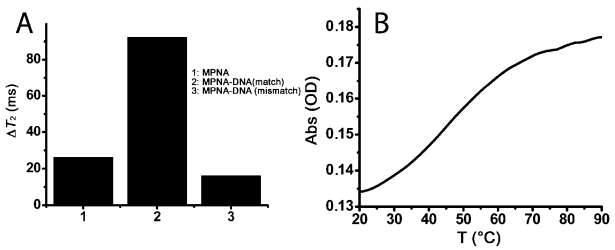

Fig. 2 Hybridization of MPNA (**13**): (A) ΔT_2 recovered in a relaxometric analysis of **13** alone (1), with matched DNA (2), mismatch DNA (3); (B) absorbance at 260 nm *vs.* temperature in a melting experiment.

Both the shape of the curve and the presence of a melting temperature (T_m = 45.8 °C, corresponding to the flex of the curve in Fig. 2B) confirm the ability of the MPNA system to recognize the complementary DNA sequence. A control experiment was performed using mismatched homo-thymine DNA, which provided no detectable binding.

These preliminary results give us confidence that our developed MPNA could be used for DNA recognition in biomedical applications.

In summary, we have developed a few practical strategies for the straightforward, efficient immobilization of PNA strands on magnetic nanoparticles. The resulting MPNA has considerable potential for biomedical application, as it can be easily manipulated and delivered to a desired target by the simple application of a controlled external electromagnetic field. Our preliminary results demonstrate that these MPNA maintain excellent performances in PNA/DNA hybridization events, which can be evidenced in a new way, through the measurement of variation of the T_2 relaxation time of water dispersions in the presence of complementary DNA. At present, the major problem concerns the solubility of these PNA-based hybrid nanostructures even if this was not an obstacle under the diluted conditions utilized for the experiments reported in this communication. Work is currently ongoing to improve the solubilization of PNA-derivatized MNP for potential use in *in vivo* experiments.

This work was supported by MIUR and University of Milan, PRIN 2007 (2007F9TWKE_002), PUR 2008, Fondazione "Romeo ed Enrica Invernizzi", and CNR-Regione Lombardia "Mind in Italy" project.

Notes and references

1 P. E. Nielsen, M. Egholm, R. H. Berg and O. Buchardt, *Science*, 1991, **254**, 1497.
2 P. Cerea, C. Giannini, S. Dall'Angelo, E. Licandro, S. Maiorana and R. Marchelli, *Tetrahedron*, 2007, **63**, 4108.
3 N. L. Rosi and C. A. Mirkin, *Chem. Rev.*, 2005, **105**, 1547.
4 S. Laurent, D. Forge, M. Port, A. Roch, C. Robic, L. Van der Elst and R. N. Muller, *Chem. Rev.*, 2008, **108**, 2064.
5 H. Gu, K. Xu, C. Xu and B. Xu, *Chem. Commun.*, 2006, 941.
6 B. Yoza, A. Arakaki, K. Maruyama, H. Takeyama and T. Matsunaga, *J. Biosci. Bioeng.*, 2003, **95**, 21.
7 M. Chorny, B. Polyak, I. S. Alferiev, K. Walsh, G. Friedman and R. J. Levy, *FASEB J.*, 2007, **21**, 2510.
8 M. G. Harisinghani, J. Barentsz, P. F. Hahn, W. M. Deserno, S. Tabatabaei, C. H. van de Kaa, J. de la Rosette and R. Weissleder, *N. Engl. J. Med.*, 2003, **348**, 2491.
9 J. P. Fortin, C. Wilhelm, J. Servais, C. Menager, J. C. Bacri and F. Gazeau, *J. Am. Chem. Soc.*, 2007, **129**, 2628.
10 L. Josephson, V. Perez and R. Weissleder, *Angew. Chem., Int. Ed.*, 2001, **40**, 3204.
11 F. Wang, H. Shen, J. Feng and H. Yang, *Microchim. Acta*, 2006, **153**, 15.
12 M. Pita, J. M. Abad, C. Vaz-Dominguez, C. Briones, E. Mateo-Martí, J. A. Martín-Gago, M. del Puerto Morales and V. M. Fernandez, *J. Colloid Interface Sci.*, 2008, **321**, 484.
13 A. P. Herrera, C. Barrera and C. Rinaldi, *J. Mater. Chem.*, 2008, **18**, 3650.
14 L. Polito, M. Colombo, D. Monti, S. Melato, E. Caneva and D. Prosperi, *J. Am. Chem. Soc.*, 2008, **130**, 12712.
15 L. Polito, D. Monti, E. Caneva, E. Delnevo, G. Russo and D. Prosperi, *Chem. Commun.*, 2008, 621.
16 M. Colombo, S. Ronchi, D. Monti, F. Corsi, E. Trabucchi and D. Prosperi, *Anal. Biochem.*, 2009, **392**, 96–102.